Available online at www.sciencedirect.com
SCIENCE DIRECT
Journal of Photochemistry and Photobiology A: Chemistry 180 (2006) 300–306
Journal of Photochemistry and Photobiology A:Chemistry
www.elsevier.com/locate/jphotochem

Discriminating bacteria from other atmospheric particles using femtosecond molecular dynamics

François Courvoisier[a,c], Véronique Boutou[a,*], Laurent Guyon[a], Matthias Roth[b], Herschel Rabitz[b], Jean-Pierre Wolf[a,c]

[a] *LASIM, UMR CNRS 5579, Université Claude Bernard Lyon 1, 43 bd du 11 Novembre 1918, F-69622 Villeurbanne Cedex, France*
[b] *Department of Chemistry, Princeton University, Frick Laboratory, Princeton, NJ 08544, USA.*
[c] *GAP-Biophotonics, Université de Genève, Rue de l'Ecole de Médecine 20, CH1211 Genève 4, Suisse*

Abstract

We investigated femtosecond pump–repump depletion schemes in biological fluorophors (tryptophan and riboflavin) in order to discriminate bioaerosols from organic interferents emitted by combustion (traffic related urban aerosols). Although fluorescence depletion is significative for riboflavin (Rbf, Vitamin B2), the most striking results have been obtained for the amino acid tryptophan (Trp). By using a 270 nm-pump 810 nm-repump femtosecond excitation, we showed that Trp exhibits fluorescence depletion up to 50%, contrary to naphthalene (<2%), despite almost identical absorption/emission spectra. We demonstrate that this process in Trp is so robust that it still occurs in living bacteria (*Bacillus subtilis*, *Escherechia coli* and *Enterococcus fæcalis*) but is absent for pure diesel fuel. This remarkable difference between biological and organic aerosols can be exploited to discriminate among them.

Keywords: Femtosecond fluorescence depletion; Aerosol particles discrimination; Bio-molecules ultrafast spectroscopy; Biological intrinsic fluorophore; Real-time particle detection

1. Introduction

Real-time detection and identification of bacteria or pollens in the air, e.g. bioaerosols, is a challenging problem to be solved for public safety requirements (legionella, SARS epidemia, allergies, bioterrorism...). Urban atmospheric aerosols (excluding water droplets from fog and clouds) generally consist of a complex mixture of mineral particles, sulphates, nitrates and a large fraction (typ. 10%–60% by mass) [1] of organic particles released by transportation vehicles, especially by diesel engines.

At the present time, bioaerosol identification is usually performed through field sampling and immunoassaying [2]. The currently available biochemical techniques, such as polymerase chain reaction (PCR) [3,4], fluorescence in situ hybridization (FISH) [5], or ultrafast B-cell adaptative immune-based sensors [6], have reduced the time needed for identification but the total assay still requires at least half an hour [6].

In contrast, fluorescence spectroscopy is real-time, can operate 24 h/day, and possibly remotely [7]. Although optical techniques can lack of specificity compared to biochemical assays, they are commonly expected to be a first alert stage, prior to more precise analysis [2,8]. Several systems have been developed to distinguish bio- from non-bio- particles, mainly through UV–vis fluorescence spectroscopy of individual particles [8–10].

Fluorescence of micro-organisms is due to intrinsic fluorophors such as amino-acids (AAs), nicotinamide adenine dinucleotide (NAD) or flavins. For instance, tryptophan (Trp) constitutes nearly 5% of the dry weight of *Bacillus subtilis* spores [11]. Fluorescence spectroscopy has the undeniable advantage to be fast and non-destructive and therefore enabling further analysis. Recently, a complete sorting system has been engineered, based on the identification of fluorescence spectra and subsequent aerodynamic deflection of single particles [12].

Another advantage of fluorescence spectroscopy is that it can be implemented for remote sensing techniques such as light detection and ranging (LIDAR) [13,14]. LIDAR allows for fast remote detection of aerosol particles and three dimensional mapping of their dispersion over several kilometres.

* Corresponding author. Tel.: +33 4 72 43 16 02; fax: +33 4 72 44 58 71.
E-mail address: boutou@lasim.univ-lyon1.fr (V. Boutou).

1010-6030/$ – see front matter © 2006 Elsevier B.V. All rights reserved.
doi:10.1016/j.jphotochem.2006.03.039

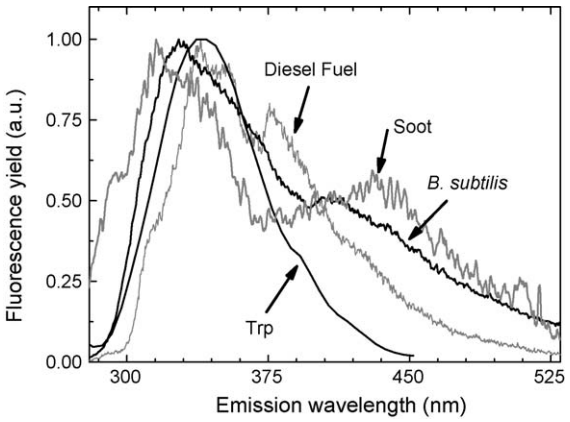

Fig. 1. Comparison of the one-photon (at 270 nm) excited fluorescence spectra for several compounds. Despite small shifts in the emission bands, an identification based on the one-photon excited fluorescence spectroscopy is impossible. Data for bacillus subtilis are shown with the courtesy of S.C. Hill (ARL).

Recently, two-photon excited fluorescence (2PEF) [7,15] has been demonstrated to remotely detect bioaerosol simulants. However, despite the success of these studies, fluorescence-based prototypes are limited by the inability of fluorescence spectroscopy to distinguish between species that have similar spectra. Although mineral and black carbon particles do not have strong fluorescence signals, aromatics and polycyclic aromatics hydrocarbons (PAHs) from organic particles and diesel soot have spectral signatures similar to biological fluorophors such as AAs [8,16]. This leads to frequent false alarms in the current field devices. The spectral similarity is attributed to the π electrons from carbonic rings which govern the spectroscopic properties (absorption and fluorescence) of PAHs, as well as biological fluorophors. Fig. 1 shows the similar fluorescence spectra of diesel fuel, soot particles and *Bacillus subtilis*, that is a biosimulant for *Bacillus anthracis*. Some small shifts in the absorption and emission bands do exist because of specific molecular skeletons, but the diverse environments of biological fluorophors in micro-organisms or the composition of PAHs in organic particles broaden and thus blur the fluorescence spectral signatures [8,16].

To overcome these difficulties, there is an interest in exciting the fluorescence with ultrafast laser pulses in order to access specific molecular dynamical features. Recent experiments using coherent control and multiphoton ultrafast spectroscopy have shown the ability to discriminate between molecular species that have similar one-photon absorption and emission spectra [17,18]. Two-photon excited fluorescence (2PEF) and pulse shaping techniques should allow for selective enhancement of the fluorescence of one molecule versus another that has similar spectra. Optimal dynamic discrimination (ODD) [19] of similar molecular agent provides the basis for generating optimal signals for detection. Recent studies emphasize that ODD could be exploited to identify bioaerosols [20,21]. This work takes advantage of the ability of molecular dynamics to give more selective information than 1PEF signals, for which molecular dynamics is averaged. Although our experiments do not strictly exploit the capabilities of ODD, it takes a first step in this direction.

2. Methodology

Fluorescence in live tissues and organisms is mainly due to the contribution of Trp and flavins [8,22]. Trp has two main absorption bands at 270 and 210 nm. Its fluorescence is widely used as a probe of protein and enzyme structure, conformational dynamics or hydratation phenomena [23]. As shown in Fig. 1, the maximum of its fluorescence is around 330 nm. Besides Trp, flavins give another large contribution to the fluorescence of bioaerosols, in particular, riboflavin (Rbf), which is a precursor of several enzymatic cofactors. It is moreover often used as a simulant of bio-particles [7,9,12,24]. Flavin mono-nucleotid (FMN) is a phosphated form of Rbf, and therefore has a higher solubility. FMN and Rbf have similar linear spectroscopic properties. Their UV–vis absorption spectrum presents three absorption bands near 405, 270 and 200 nm [25] and the maximum of its fluorescence spectrum is at 530 nm [24].

Consequently, in order to investigate the possibility to discriminate bio- and non-bio-particles based on molecular dynamics, we have chosen to study the dynamics of these main fluorophors. The spectroscopic scheme used to study both flavins and Trp is very similar but takes into account the specific absorption properties of each species. As mentioned previously, the absorption bands of naphthalene, which is one of the fluorescing PAHs in diesel fuel [26], and Trp are superimposable [25]. Therefore, prior to direct experiments with live micro-organisms and fuel, we have chosen to further compare the dynamics of Trp and naphthalene.

Following the well-known double excitation pulses spectroscopic methods [27,28], the molecular dynamics of the first excited state S_1 of these fluorescent molecules is investigated here with the following methodology. As sketched on Fig. 2, a first femtosecond pump pulse (at 270 nm for Trp and naphthalene, 405 nm for Rbf and FMN), resonant with the first absorption band of the fluorophores, coherently excites them from the ground state S_0 to a set of vibronic levels $S_1\{\nu'\}$. The vibronic excitation relaxes by internal energy redistribution to lower $\{\nu\}$ modes. Fluorescence relaxation to the ground state occurs within a lifetime of several nanoseconds (2.6 ns for Trp [29], 5 ns for Rbf [30]). Meanwhile, a second 810 nm femtosecond repump pulse is used to transfer part of the $S_1\{\nu\}$ population to higher lying electronic states S_n. The depletion of the S_1 population under investigation depends on both the molecular dynamics in this intermediate state and the coupling efficiency to S_n. The relaxation of the excitation from the S_n states may be associated with many different processes, including charge transfer, conformational relaxation (for Trp see [31,32]) and intersystem crossing with repulsive $\pi\sigma^*$ states [33,34].

In order to compare the difference in the dynamics of the biological molecules, we have used a double pump scheme, similar to the one for Trp, for Rbf and FMN. In this latter case, to bring the molecules to the first excited state S_1, a first 405 nm femtosecond pump pulse is used whereas the second pump pulse wavelength at 810 nm remains unchanged and is used to transfer a fraction of the S_1 population to the second absorption band (around 270 nm, see Fig. 2(a)) via a one-photon transition or to

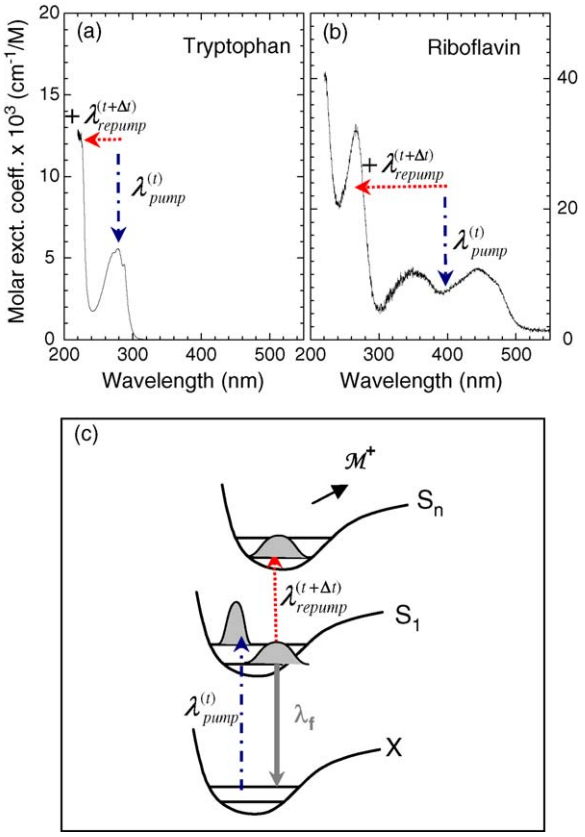

Fig. 2. Absorption spectra of Tryptophan (a) and Riboflavin (b). (c) Pump–repump excitation scheme in Trp, flavins and polycyclic aromatics. The pump pulse brings the molecules in their first excited state S_1. The S_1 population is depleted by the repump pulse.

the third one (around 200 nm, see Fig. 2(a)), via a two-photon transition.

3. Experimental set-up

The experiments use a Kerr lens mode locked Ti:sapphire oscillator followed by a chirped pulse amplifier that delivers 120 fs pulses at 810 nm. The output is frequency doubled and tripled in two consecutive crystals of β-barium borate (BBO) so that the pulses at 270 nm for Trp, Naphthalene and diesel (resp. 405 nm for Rbf and FMN) and at 810 nm are synchronously emitted. After splitting both pulses on a dichroic mirror, the near infrared repump pulse is delayed using a stepper motorized delay line, with a resolution of 16 fs. Both beams are then recombined, carefully spatially superimposed and focused onto a 1 mm quartz flow cell, leading to intensities up to $I_{270} = 4 \times 10^5$ W/cm^2 (resp. $I_{405} = 9 \times 10^8$ W/cm^2) and $I_{810} = 2 \times 10^{11}$ W/cm^2.

The fluorescence is dispersed by a low resolution Jobin Yvon Y10 spectrometer (2 nm resolution) centred at 340 nm which is close to the maximum intensity of Trp and PAH fluorescence spectra (or at 530 nm for flavins) and recorded via a photomultiplier tube. Scattering from the 270 nm beam (resp. 405 nm beam) is blocked using a dichroic mirror (high reflectivity at 270 nm, resp. at 405 nm) and a bandpass filter centered at 340 nm (FWHM 10 nm, resp. 530 nm FWHM 10 nm). The Trp or flavins are solvated in water whereas the hydrophobic naphthalene is dissolved in cyclohexane. The concentrations used are typically 0.2 g L^{-1} for Trp, 0.3 g L^{-1} for naphthalene, 0.1 g L^{-1} for Rbf and from 0.1 to 1 g L^{-1} for FMN. We have checked that our results do not depend on the different solution concentrations. In further experiments, solutions of bacteria (*Escherichia coli*, *Bacillus subtilis*, *Enterococcus fæcalis* from Symbioflor) have been prepared by dissolving lyophilized cells and spores in water (Strain W ATCC 9637 for *Escherichia coli,* ATCC 6633 for *Bacillus subtilis*) or in a nutrient buffered (Symbioflor for *Enterococcus fæcalis*) solution at concentrations of 10^7 to 10^9 bacteria/cm^3. Diesel fuel has also been used to simulate the complex mixture of PAHs contained by organic particles emitted by diesel engines. A circulator ensures that solutions in the excitation volume are fresh for each laser pulse.

4. Comparison of fluorescence depletion between tryptophan and PAHs containing samples

Fig. 3 compares the fluorescence intensity as a function of pump (270 nm)–repump (810 nm) delay for a solution of Trp and a solution of naphthalene. Whereas a strong fluorescence depletion dependent on the 810 nm pulse intensity and on the precise superimposition of pump and repump beams (fluorescence depletion can reach 50%) shows up for Trp, the fluorescence level of naphthalene remains almost unchanged even for long delays (up to 50 ps, limited by our delay line). This remarkable difference in the excited-states dynamics between Trp and naphthalene allows for their efficient discrimination, although they exhibit very similar linear absorption/fluorescence spectra [8,16].

Several groups have previously observed fluorescence depletion for aqueous Trp in the nanosecond and picosecond regime [22,35]. The authors attributed the depletion to autoionization from the S_n states. By tuning their excitation wavelength from 270 to 220 nm, they showed a decrease of the Trp quantum yield

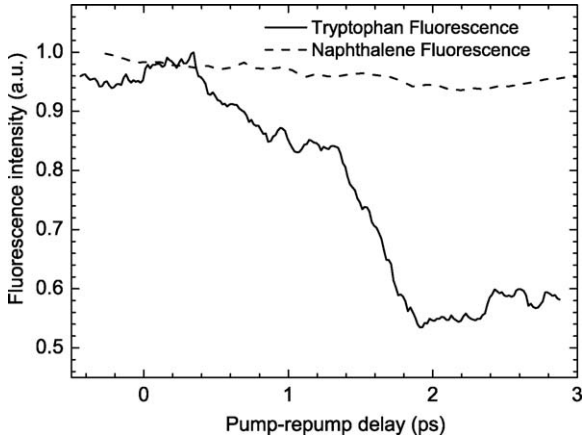

Fig. 3. Fluorescence intensity as a function of pump–repump delay for Trp (solvated in water) to simulate micro-organisms and a PAH, naphthalene (in cyclohexane) to simulate organic fluorescent particles. The fluorescence of Trp exhibits a strong depletion whereas almost no extinction is visible for naphthalene despite very similar one-photon absorption and fluorescence spectra. Time origin is arbitrary.

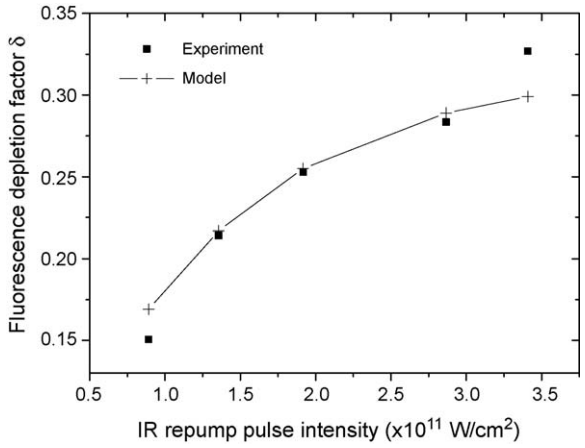

Fig. 4. Trp fluorescence depletion factor δ, as a function of the near IR repump pulse intensity. Comparison between experimental data and a fit obtained using the 3-level model described in the text. Noise, especially due to laser fluctuations and to pump–repump alignment in the experiment is responsible for a 3–5% error on each point.

of 30–50% while the Trp photoionization increased [36,37]. Calculations of the molecular dynamics of Trp on the S_n surface including solvent interactions are, however, needed to fully interpret this depletion feature.

Fig. 4 shows the variation of the relative fluorescence depletion $\delta = (F_{\text{undepleted}} - F_{\text{depleted}})/F_{\text{undepleted}}$ as a function of the repump pulse intensity. As recently demonstrated by Iketaki et al. [35], the fluorescence depletion can be described in a simple three states model S_0, S_1, S_n, where a portion, α, of the S_n population does not relax on S_1, i.e. does not give rise to fluorescence. The rate equations of the three populations N_0, N_1 and N_n of the respective states S_0, S_1, S_n are written as:

$$\frac{dN_0}{dt} = -\sigma_0 I_{270} N_0 + \frac{1}{\tau} N_1;$$

$$\frac{dN_1}{dt} = \sigma_0 I_{270} N_0 - \left(\frac{1}{\tau} + \sigma_1 I_{810}\right) N_1 + k_{n1} N_n;$$

$$\frac{dN_n}{dt} = \sigma_1 I_{810} N_1 - (k_{\text{loss}} + k_{n1}) N_n$$

where σ_0 and σ_1 are respectively the one-photon transition cross sections at 270 and 810 nm; τ is the lifetime in the S_1 state; k_{n1} and k_{loss} are the relaxation rates corresponding to the transitions from S_n, respectively to S_1 and non-fluorescing states (e.g. triplet states, ionization, non-radiative decay, etc.). In the model, following [35], we used $\sigma_0 = 10^{-17}$ cm^2 (at a wavelength of 270 nm), $\sigma_1 = 10^{-17}$ cm^2 (at a wavelength of 810 nm), $\tau = 2.6$ ns and $k_{n1} = 10^{11}$/s.

The branching ratio to non-fluorescing states, α, is defined by:

$$\alpha = \frac{k_{\text{loss}}}{k_{\text{loss}} + k_{n1}}$$

where k_{loss} is the unknown parameter.

The model fits the experimental power dependence well and indicates that the transition $S_1 \rightarrow S_n$ requires only one photon. The best fit of the experimental data was obtained for $\alpha \approx 30\%$ (black curve of Fig. 4). This value of α is in agreement with previous measurements of photoionization [36], laser flash photolysis [38] or Raman UV spectroscopy [22]. Concerning the power dependence with respect to the first pump pulse incident intensity upon the depletion efficiency, we have verified experimentally that it remains in the linear regime. However, this kinetic model does not explain the dynamics on S_1 observed on the picosecond scale (Fig. 3) and further analysis is required to fully interpret the depletion curve.

In contrast with tryptophan, the absence of fluorescence depletion for naphthalene in cyclohexane may be attributed to the difference in ionization potential. In the gaseous phase, the ionization potential of naphthalene is about 1 eV higher than Trp [39], and a similar difference might be expected in the liquid phase.

5. Pump–repump fluorescence depletion in flavins

Fig. 5 shows the fluorescence intensity of FMN as a function of the time delay between the 405 nm pump and 810 nm repump pulses. As in the Trp case, FMN undergoes fluorescence depletion. We have repeated this experiment with Rbf which showed no noticeable differences with FMN.

Fig. 6 shows the dependency of the fluorescence depletion of FMN on the 810 nm repump pulse intensity. For this study, FMN was preferred to Rbf because of its higher solubility. The power dependence upon the near IR pulse is 1.4, which indicates that the depletion process is likely to be due to a combination of a one- and a two-photon transition. Indeed, FMN absorption spectrum (Fig. 2(b)) presents two absorption bands that are resonant with the absorption of one or two photons at 810 nm from S_1.

Numerical simulations have then been performed with a three state model. As shown in Fig. 6, fits in fair agreement with the experimental data can be obtained for both the one-photon and two-photon transition assumptions. For the two-photon

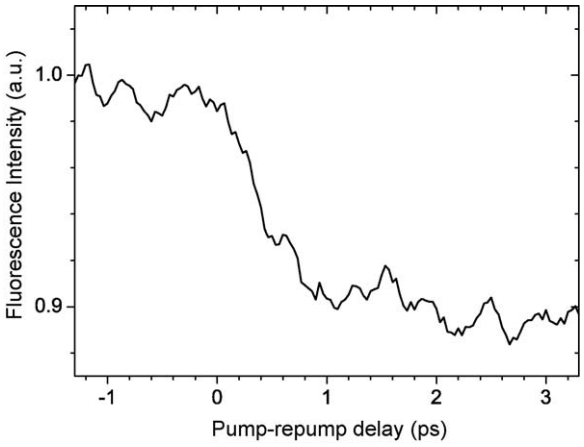

Fig. 5. Fluorescence intensity as a function of time delay Δt between the first pump (at 405 nm) and the repump (at 810 nm) pulses for a solution of FMN. As for Trp, an extinction of the fluorescence due to the repump pulse is clearly visible. The same evolution has also been observed for riboflavin. The maximum depletion for Rbf or FMN is smaller (not more than 25%) than for Trp. The repump intensity required is an order of magnitude higher than for Trp. Fluctuations on the fluorescence signal of FMN are due to laser noise.

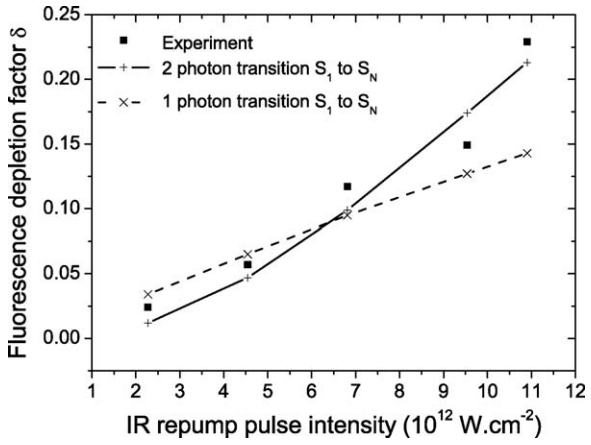

Fig. 6. FMN fluorescence depletion factor δ as a function of the near IR repump pulse intensity. Comparison between experimental data and the result of two fits assuming a 3-level rate equation model. For both one- ($S_1 \rightarrow S_n$) and two-photon ($S_1 \rightarrow S_n$') transition, good agreement is obtained with experimental data, for which a power dependence exponent of 1.4 with respect to the near IR pulse intensity is observed. This behaviour might explain the higher repump pulse intensity required for fluorescence depletion in flavins.

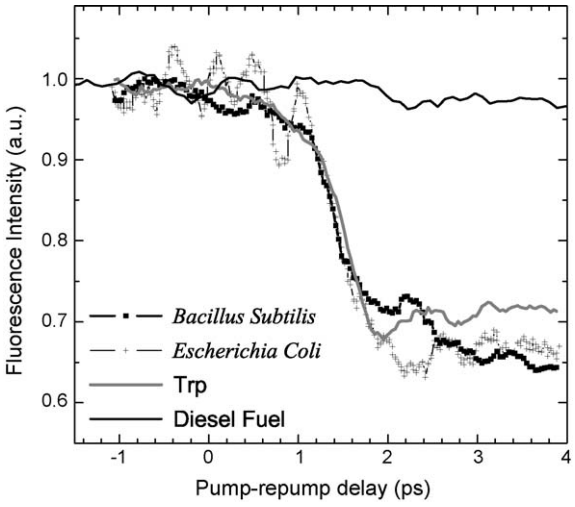

Fig. 7. Fluorescence intensity as a function of pump–repump time delay for several micro-organisms (in solution) compared to Trp in water and to diesel fuel (to simulate fluorescence organic particles). The striking feature is that even for Trp embedded in a complex proteinic environment, a strong extinction of the fluorescence is observed whereas no depletion (higher than a few percent) occurs for diesel fuel. Discrimination between bio- and organic fluorescent particles based on pump–repump depletion spectroscopy is therefore possible.

transition, we simply modified $\sigma_1 I_{810}$ in the 3-level model used for Trp by $\sigma_1' I_{810}^2$, where σ_1' is a two-photon cross-section. The parameters used are then $\sigma_0 = 0.4 \times 10^{-16}$ cm^2, $\sigma_1 = 1.0 \times 10^{-16}$ cm^2, $k_{n1} = 1.7 \times 10^{13}$ s^{-1} [30]. For the two-photon absorption cross section from S_1, we assumed that it is the same as from S_0: $\sigma_1' = 0.4 \times 10^{-50}$ cm^4 s/photon [40]. In both cases, the value of the branching ratio to non-fluorescing states, α, is about 0.3. However, to get a reasonable fit for a one-photon transition, a correction factor of 10^{-2} on the near IR pulse intensity was needed. Because measurement error of the intensity cannot be so high, this situation may reflect that the fluorescence depletion of Rbf and FMN is mainly due to a two-photon transition from S_1 to S_n'. A more precise analysis of the branching ratios would require the exact transition cross-section between excited states, which is yet unknown to our knowledge.

We can moreover notice that the 810 nm repump pulse intensity required to efficiently deplete the fluorescence of Rbf is about one order of magnitude higher than for Trp. This result can be explained by the two-photon transition from S_1 to higher excited states in the case of Rbf, contrary to the one-photon transition in the case of Trp.

An interesting suggestion arising from this study would be to test the dynamics of Rbf and FMN if the pump pulse is for both molecules at 270 nm, in order to compare the depletion efficiency with the (405 nm + 810 nm) excitation.

6. Pump–repump depletion-based discrimination between bio- and non-bio- particles

The excited state dynamics of bio- (especially Trp) and non-bio-fluorophors are significantly different, which allows their discrimination, despite almost identical linear absorption/emission spectra. In order to determine how this approach applies to the discrimination of bioagents from organic particles, the 270 nm pump–810 nm repump experiment was repeated with live bacteria in solution: *Enterococcus fæcalis*, *Escherechia coli* (simulant of *Yersinia pestis*) and *Bacillus subtilis* (simulant of *Bacillus anthracis*).

Fig. 7 compares the fluorescence intensity of *B. subtilis*, *E. coli*, free Trp and pure diesel fuel as a function of the pump–repump delay. The fluorescence depletion in Trp is so robust that even in the case of highly complex systems like bacteria, the process is preserved. All three curves presented in Fig. 7 are obtained under the same experimental conditions. Results for *Enterococcus fæcalis*, not shown here, are similar. Note that the small oscillations observed on the curve of *E. coli* are not reproducible.

In contrast with the amino-acids, the complex mixture of PAHs in pure diesel fuel does not show up any significant fluorescence depletion (not more than 2%), as for naphthalene. This remarkable depletion process observed for Trp in bacteria allows us to introduce a novel scheme in order to discriminate between micro-organisms and their main masking agent in air, namely organic particles.

The Trp fluorescence depletion is proportional to the S_1 population decrease through the transfer to S_n. As already mentioned, a linear dependency of the depletion on the 270 nm pump pulse intensity I_{270} is expected if saturation of the transition $S_0 \rightarrow S_1$ is avoided. In our case, I_{270}^{sat} would be 5.10^{11} W/cm^2 which is well beyond the intensity used in the experiment: $I_{270} = 4 \times 10^5$ W/cm^2. In this linear regime, the fluorescence due to the 270 nm pulse excitation is proportional to $F = \sigma I_{270}$, with σ, the fluorescence cross section. If the excitation consists of a 270 nm pump pulse followed by a 810 nm repump pulse, an effective fluorescence cross section can be introduced $R \times \sigma$, where R is the depletion factor and depends on the bio- or non-

bio- nature of the particle. This factor can be as low as 0.5 for bacteria whereas it remains about 1 for PAHs containing particles.

Therefore, to address the bio- or non-bio- nature of a single unknown aerosol particle, we propose a setup which consists of a two-step interrogation of its fluorescence: (1) a single UV femtosecond pump pulse excitation that leads to the fluorescence signal $F_{off} = \sigma I_{270}$ and (2) a UV pump pulse followed by a 810 nm repump pulse excitation that leads to the signal $F_{on} = R \times \sigma I_{270}$. A direct comparison of F_{on} and F_{off} then allows for discrimination. In the case of single particle analysis [8,12], if $F_{on} = F_{off}$, the particule would be organic, whereas if F_{on} is smaller than F_{off}, it would be most likely a bacteria signal. The different behaviour between bio- and non-bio- particles could also be used to remotely identify bioaerosol particles in a LIDAR configuration. In that case, the detectability threshold may vary because of the large size range of organic particles. In addition, polluted urban atmospheres can reach a ratio of about 1 bio-particle for 10^3 background particles [12]. In order to reach such a high detection ratio, further enhancement of the R factor between these species will be needed, but this may require more sophisticated excitation schemes such as optimal dynamic discrimination (ODD).

7. Conclusion

This work reports a pump–repump depletion study of the main fluorophors of bioaerosols (Trp, Rbf) and organic particles (naphthalene). We showed that they exhibit very different behaviours: Trp undergoes a strong fluorescence depletion whereas no depletion is observable for naphthalene. The most remarkable result is that this difference is transposable to the case of a solution of living bacteria and pure diesel fuel. This opens up a new mean of discrimination between bioaerosols and organic aerosols although they are undistinguishable with linear UV–vis spectroscopy. A further step would be to repeat these experiments with aerosolized bacteria and transportation soot particles emitted from diesel engines.

Recently, optimal dynamic discrimination and coherent control have theoretically proven to be efficient in such cases of discrimination between several species in a mixture [20]. Based on this and on previous experiments, we plan to focus future studies on identifying the best ODD schemes in order to discriminate between bio- and non-bio- aerosols, and eventually between different bioaerosols.

Acknowledgements

J.-P.W. thanks P. Callis, S.C. Hill and P. Hargis for fruitful discussions. F.C., V.B., and J.-P.W. acknowledge DGA's grant 036000036004707501 and la Région Rhône-Alpes for its support through *Emergence*. H.R. acknowledges the support of the Army Research Office and the DoD Multidisciplinary University Research Initiative Program. J-P.W. acknowledges NATO's grant SSTCLG977928.

References

[1] J. Seinfeld, S. Pandis, Atmospheric Chemistry and Physics, E.W. Sons (ed.), New York, 1998.
[2] J. Ho, Anal. Chim. Acta 457 (2002) 125.
[3] P.R. Murray, E.J. Baron, L.A. Pfaller, Manual of Clinical Microbiology, American Society for Microbiology, New York, 2003.
[4] P. Belgrader, W. Bennett, D. Hadley, J. Richards, P. Stratton, R. Mariella, F. Milanovich, Science 284 (1999) 449.
[5] B. Beatty, S. Mai, J. Squire, FISH: A Practical Approach, Oxford University Press, London, 2002.
[6] T.H. Rider, M.S. Petrovick, F.E. Nargi, J.D. Harper, E.D. Schwoebel, R.H. Mathews, D.J. Blanchard, L.T. Bortolin, A.M. Young, J.Z. Chen, M.A. Hollis, Science 301 (2003) 213.
[7] G. Méjean, J. Kasparian, J. Yu, S. Frey, E. Salmon, J.-P. Wolf, Appl. Physics B 78 (2004) 535.
[8] S.C. Hill, R.G. Pinnick, S. Niles, Y.-L. Pan, S. Holler, R.K. Chang, J. Bottiger, B.T. Chen, C.-S. Orr, G. Feather, Field Anal. Chem. Technol. 3 (4–5) (1999) 221.
[9] F.L. Reyes, T.H. Jeys, N.R. Newbury, C.A. Primmerman, G.S. Rowe, A. Sanchez, Field Anal. Chem. Tech. 3 (1999) 240.
[10] J.D. Eversole, W.K. Cary, C.S. Scotto, R. Pierson, M. Spence, A.J. Campillo, Field Anal. Chem. Tech. 5 (2001) 205.
[11] G.W. Faris, R.A. Copeland, K. Mortelmans, B.V. Bronk, Appl. Optics 36 (4) (1997) 958.
[12] Y.-L. Pan, V. Boutou, J.R. Bottiger, S.S. Zhang, J.-P. Wolf, R.K. Chang, Aerosol Sci. Technol. 38 (6) (2004) 598.
[13] R.M. Measures, Laser Remote Sensing, E.J.W. Sons (ed.), New York, 1984.
[14] J.P. Wolf, UV-DIAL-Lidar Techniques for Air Pollution Monitoring, in: E.R.A. Meyers (Ed.), Encyclopedia of Analytical Chemistry, J. Wiley & Sons, New York, 2000, p. 2226.
[15] J. Kasparian, M. Rodriguez, G. Méjean, J. Yu, E. Salmon, H. Wille, R. Bourayou, S. Frey, Y.-B. André, A. Mysyrowicz, R. Sauerbrey, J.-P. Wolf, L. Wöste, Science 301 (2003) 61.
[16] R.G. Pinnick, S.C. Hill, Y.L. Pan, R.K. Chang, Atmospheric Environ. 38 (2004) 1657.
[17] T. Brixner, N.H. Damrauer, P. Niklaus, G. Gerber, Nature 414 (2001) 57.
[18] K.A. Walowicz, I. Pastirk, V.V. Lozovoy, M. Dantus, JPCA 106 (41) (2002) 9369.
[19] B. Li, G. Turinici, V. Ramakrishna, A.H. Rabitz, J. Phys. Chem. B 106 (2002) 8125.
[20] B. Li, H. Rabitz, J.P. Wolf, J. Chem. Phys. 122 (2005) 154103.
[21] M.O. Scully, G.W. Kattawar, R.P. Lucht, T. Opartny, H. Pilloff, A. Rebane, A.V. Sokolov, A.M.S. Zubairy, PNAS 99 (17) (2002) 10994.
[22] J.P. Teraoka, A. Harmon, S.A. Asher, J. Am. Chem. Soc. 112 (1989) 2892.
[23] S.K. Pal, J. Peon, A.H. Zewail, Chem. Phys. Lett. 363 (1–2) (2002) 57.
[24] Y.-L. Pan, R.G. Pinnick, S.C. Hill, S. Niles, S. Holler, J.R. Bottiger, J.P. Wolf, R.K. Chang, Appl. Phys. B 72 (2001) 449.
[25] photoChemCAD, http://omlc.ogi.edu/spectra/PhotochemCAD/html/.
[26] E. Leotz-Gartziandia, V. Tatry, P. Carlier, Environ. Monitoring Assessment 65 (2000) 155.
[27] M. Yan, L. Rothberg, R. Callender, J. Phys. Chem. B 105 (2001) 856.
[28] F. Gai, J. Cooper Mc Donald, P.A. Anfinrud, J. Am. Chem. Soc. 119 (1997) 6201.
[29] R.W. Wijnaendts van Resandt, R.H. Vogel, S.W. Provencher, Rev. Sci. Instrum. 53 (1982) 1392.
[30] S.D.M. Islam, A. Penzkofer, P. Hegemann, Chem. Phys. 291 (2003) 97.
[31] J.T. Vivian, P.R. Callis, Biophys. J. 80 (2001) 2093.
[32] P.R. Callis, J.T. Vivian, Chem. Phys. Lett. 369 (2003) 409.
[33] C. Dedonder-Lardeux, C. Jouvet, S. Perun, A.L. Sobolewski, Phys. Chem. Chem. Phys. 5 (2003) 5118.
[34] A.L. Sobolewski, W. Domcke, C. Dedonder-Lardeux, A.C. Jouvet, Phys. Chem. Chem. Phys. 4 (2002) 1093.

[35] Y. Iketaki, T. Watanabe, S.-i. Ishiuchi, M. Sakai, T. Omatsu, K. Yamamoto, M. Fujii, A.T. Watanabe, Chem. Phys. Lett. 372 (2003) 773.
[36] H.B. Steen, J. Chem. Phys. 61 (10) (1974) 3997.
[37] I. Tatischeff, R. Klein, Photochem. Photobiol. 22 (1975) 221.
[38] J.C. Mialocq, E. Amouyal, A. Bernas, D. Grand, J. Phys. Chem. 86 (1982) 3173.
[39] http://webbook.nist.gov/cgi/cbook.cgi%3FID=C91203%26Units=SI%26Mask=20.
[40] G.A. Blab, P.H.M. Lommerse, L. Cognet, G.S. Harms, T. Schmidt, Chem. Phys. Lett. 350 (2001) 71.